

## Divalent Rare-Earth Ions in LaF<sub>3</sub> Crystals

E. A. Radzhabov<sup>a, b, \*</sup> and A. V. Samborsky<sup>b</sup>

<sup>a</sup>Vinogradov Institute of Geochemistry, Siberian Branch, Russian Academy of Sciences, Irkutsk, 664033 Russia

<sup>b</sup>Irkutsk State University, Irkutsk, 664003 Russia

\*e-mail: eradz@igc.irk.ru

**Abstract**—The optical spectra and electric conductivity of LaF<sub>3</sub> crystals doped with 0.01, 0.1, and 0.3 mol % YbF<sub>3</sub>, where Yb was partly or completely recharged to the divalent state, are studied. The long-wavelength absorption band of 370 nm is caused by electrons transitioning from state  $4f^{14}$  to the level of anion vacancies. The remaining bands at 300–190 nm are caused by  $4f^{14}-5d^14f^{13}$  transitions in Yb<sup>2+</sup>. The bulk electric conductivity and peaks of the dielectric losses of LaF<sub>3</sub>–Yb<sup>2+</sup> crystals are caused by Yb<sup>2+</sup>–anion vacancy dipoles. The activation energy of the reorientation of Yb dipoles is 0.58 eV. The optical and dielectric properties of Yb<sup>2+</sup> centers are compared to those of Sm<sup>2+</sup> and Eu<sup>2+</sup> centers studied earlier in LaF<sub>3</sub> crystals.

DOI: 10.3103/S1062873817090209

### INTRODUCTION

Optical spectra of trivalent rare-earth (RE<sup>3+</sup>) ions in LaF<sub>3</sub> crystals were studied in detail in the 1980s [1]. The  $f$ – $d$ -interconfiguration and  $f$ – $f$ -intraconfiguration spectra of divalent RE ions were thoroughly studied in crystals of alkaline earth fluorides [2, 3]. At the same time, spectroscopy of these ions in LaF<sub>3</sub> remains poorly studied. According to absorption spectra induced by X-ray radiation, Nd, Sm, Tm, and Yb ions partially transform into a divalent state [4]. The concentration of radiation centers is low, however, and prevents study of the dielectric properties of crystals reduced by radiation. In this work, we studied the spectra of Yb<sup>2+</sup>-doped (and Sm<sup>2+</sup>- and Eu<sup>2+</sup>-doped [5, 6]) LaF<sub>3</sub> crystals, in which these divalent ions are obtained by selecting the conditions of growth in concentration sufficient for both optical and dielectric measurements.

### EXPERIMENTAL

LaF<sub>3</sub> crystals were grown using the Stockbarger technique in a three-barreled graphite crucible in a vacuum. Several percents of CdF<sub>2</sub> were added to remove any oxygen. The REF<sub>3</sub> contents in the charges of each series were 0.01, 0.1, and 0.3 mol %. We grew crystals that contained only RE<sup>3+</sup>, along with crystals containing some trivalent Sm and Yb ions brought to the divalent form. The Eu ions were only in the divalent form. Due to absorption bands in the visible area, the LaF<sub>3</sub> crystals with divalent RE ions were greenish (LaF<sub>3</sub>–Sm<sup>2+</sup>) and yellowish (LaF<sub>3</sub>–Eu<sup>2+</sup> and LaF<sub>3</sub>–Yb<sup>2+</sup>). According to preliminary data, adding an excess amount of CdF<sub>2</sub> reduces initially trivalent

REEs. We grew crystals with trivalent (LaF<sub>3</sub>–YbF<sub>3</sub>(Yb<sup>3+</sup>)) and partly or completely divalent (LaF<sub>3</sub>–YbF<sub>3</sub>(Yb<sup>2+</sup>/Yb<sup>3+</sup>) and LaF<sub>3</sub>–YbF<sub>3</sub>(Yb<sup>2+</sup>)).

The absorption spectra were measured on a Lambda-950 spectrophotometer (PerkinElmer) in the range of 190–3000 nm. Luminescence and vacuum UV spectra were registered on a laboratory device using BMP2 (115–300 nm) and MDR2 monochromators, a L7292 discharge deuterium lamp (Hamamatsu) as a source of vacuum ultraviolet, and a FEU142 radiation detector. Spectra in the range of 200–850 nm were measured using a Hamamatsu H6780-04 photomodule.

Electrodes were covered in silver (Kettler epoxy). They were ~5 mm in diameter at a sample thickness of ~2 mm. Electrical conductivity with alternating current was measured using an E7-20 (MNIPI) immitance tester in the frequency range of 25 Hz–1 MHz at temperatures of 77–400 K. The unit for measuring conductivity was the Siemens (S), i.e., Ω<sup>-1</sup>.

### RESULTS

#### Optical Spectra

Yb<sup>3+</sup>-doped crystals have no absorption bands in visible spectrum range [7] and contain weak bands near 970 nm caused by  $^2F_{7/2}-^2F_{5/2}$  transitions [8]. There are no bands at ~970 nm in crystals with divalent Yb, in contrast to those in the UV range of the spectrum (450–200 nm) (Fig. 1). The UV bands in LaF<sub>3</sub>–YbF<sub>3</sub>(Yb<sup>2+</sup>) crystals (and in LaF<sub>3</sub>–YbF<sub>3</sub>(Yb<sup>2+</sup>/Yb<sup>3+</sup>) crystals of the same series) grow along with the YbF<sub>3</sub> concentration (Fig. 1). At low temperatures, the

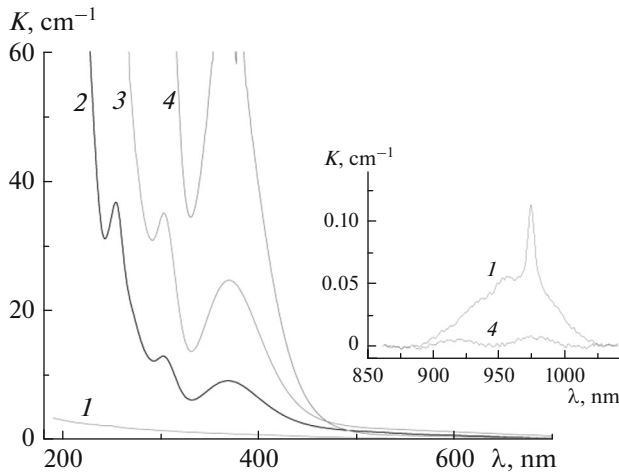


**Fig. 1.** Absorption spectra of LaF<sub>3</sub> crystals with (1) 0.3, (2) 0.01, (3) 0.1, (4) 0.3% YbF<sub>3</sub> at room temperature. Yb was trivalent in crystal (1); it was divalent in the other crystals. The insert shows the absorption spectra of the crystals in the range of the  ${}^2F_{7/2}-{}^2F_{5/2}$  transition of trivalent Yb.

absorption spectra of LaF<sub>3</sub>–Yb<sup>2+</sup> become more detailed, with bands at 377, 301, 254.7, 221.5, and 201 nm (Fig. 2). When the temperature falls, the Yb<sup>2+</sup> bands shift toward the short-wavelength range, displacing a band at ~370 nm, which shifts toward the long-wavelength range. X-ray irradiation of LaF<sub>3</sub>–Yb<sup>3+</sup> crystals reduces the amount of Yb to Yb<sup>2+</sup>, as can be seen from the coincident absorption spectra (Fig. 2).

The concentration dependence of the absorption coefficient in the maximum of the long-wavelength band is linear (Fig. 2, insert). The crystals with incomplete reduction of trivalent Yb exhibit similar concentration dependences (Fig. 2, insert). The straight lines do not converge at the origin. The initial material was probably partly mixed in a three-barreled crucible upon vacuumization. The ratio of the concentration of divalent Yb in LaF<sub>3</sub> according to the long-wavelength absorption band at 370 nm was  $C$  (mol %) =  $k_{360 \text{ nm}} (\text{cm}^{-1})/193 (\text{cm}^{-1} \text{ mol } \%^{-1})$ , suggesting that the highest YbF<sub>3</sub> concentration of 0.3 mol % changed slightly as the crystals grew.

This ratio can be rewritten as  $N (\text{cm}^{-3}) = k (\text{cm}^{-1})/\sigma (\text{cm}^2)$ , where  $N$  is the concentration per cubic centimeter and  $\sigma$  is the cross-section of the absorption band.

The coefficient  $\sigma$  in LaF<sub>3</sub>–Yb<sup>2+</sup> crystal for the 370- and 304-nm bands was thus  $6.3 \times 10^{-18}$  and  $9.4 \times 10^{-18} \text{ cm}^2$ , respectively. The concentration ratio was  $N (\text{cm}^{-3}) = k_{370 \text{ nm}} (\text{cm}^{-1})/6.3 \times 10^{-18} \text{ cm}^2$ .

In [9], the absorption cross-section  $\sigma$  for CaF<sub>2</sub>–Yb<sup>2+</sup> in a 365-nm band was taken to be  $7.4 \times 10^{-18} \text{ cm}^2$ .

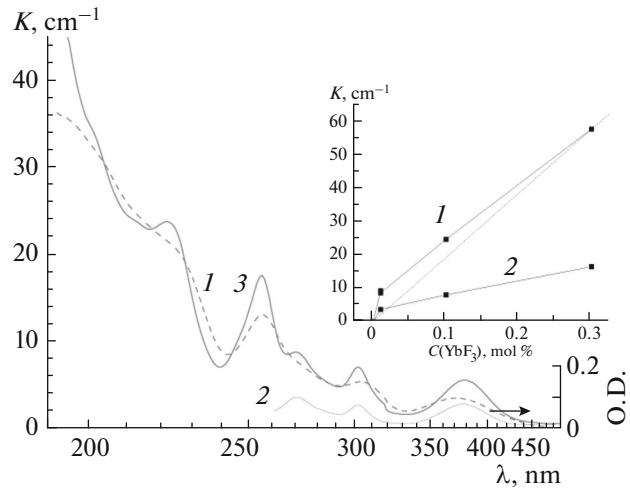


**Fig. 2.** Absorption spectra of LaF<sub>3</sub>–YbF<sub>3</sub>(Yb<sup>2+</sup>/Yb<sup>3+</sup>) crystals. In crystals (1) 0.01% YbF<sub>3</sub> at  $T = 295 \text{ K}$  and (3) 0.01% YbF<sub>3</sub> at  $T = 7.4 \text{ K}$ , Yb is partly reduced to the divalent state as they grow. In crystals (2) 0.3% YbF<sub>3</sub> at  $T = 7.5 \text{ K}$ , Yb<sup>2+</sup> ions are formed by X-ray radiation at room temperature. The insert shows the concentration dependence of the optical absorption band of LaF<sub>3</sub> crystals at 370 nm with (1) full and (2) partial reduction of Yb to the divalent state. The dotted line shows the corrected concentration dependence.

It should be noted that the band at 365 nm in CaF<sub>2</sub> was caused by  $4f^{14}-4f^{13}5d^1$  transitions in Yb<sup>2+</sup>; judging from the type of transitions in LaF<sub>3</sub>–Yb<sup>2+</sup>, it corresponded to the band at 304 nm (at room temperature), the value of which is slightly higher than that of the long-wavelength band at 370 nm (Figs. 1, 2) and  $\sigma = 9.4 \times 10^{-18} \text{ cm}^2$ . The absorption cross-section for the first band of  $4f^{14}-4f^{13}5d^1$  Yb<sup>2+</sup> in CaF<sub>2</sub> [9] and LaF<sub>3</sub> are close in value.

### Electrical Conductivity

The complex conductivity of LaF<sub>3</sub>–Yb<sup>2+</sup> (Fig. 3) is described by an equivalent chain composed of frequency-dependent capacity ( $C_p$ ) and frequency-independent active resistance ( $R$ ) connected in parallel [10]. Similar dependences of complex conductivity were measured for LaF<sub>3</sub>–Sm<sup>2+</sup> [5], LaF<sub>3</sub>–Eu<sup>2+</sup> [6], and LaF<sub>3</sub>–Ba<sup>2+</sup> in [11]. At low frequencies, the conductivities approached zero. For an ideal chain, the intersection of the curve of complex conductivity and axis  $x$  at high frequencies yields the correct value of bulk active conductivity (below, conductivity) of a crystal [11, 12]. The conductivity of LaF<sub>3</sub> grows along with the concentration of Yb<sup>2+</sup> (Fig. 3). As with Sm<sup>2+</sup> [5] and Eu<sup>2+</sup>, there is also a linear correlation between the conductivity and optical absorption of Yb<sup>2+</sup> in

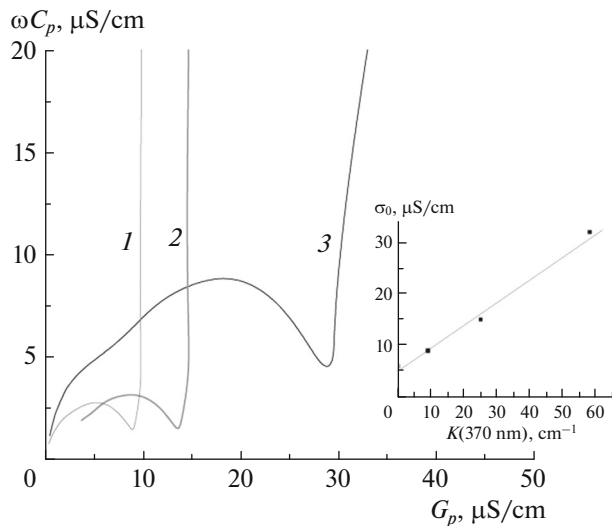


**Fig. 3.** Spectra of the complex conductivity of  $\text{LaF}_3\text{-YbF}_3$  ( $\text{Yb}^{2+}$ ) crystals at room temperature: (1) 0.01, (2) 0.1, (3) 0.3 mol %  $\text{Yb}^{2+}$ . The point of intersection with axis  $x$  yields the active conductivity of the crystal [9, 10]. The insert shows the correlation between specific active conductivity  $\sigma_0$  and absorption coefficient  $K$  of the long-wavelength band of  $\text{Yb}^{2+}$  centers at 370 nm.

$\text{LaF}_3$  (insert in Fig. 3) [6]. This testifies to the direct interrelation between dipoles and  $\text{Yb}^{2+}$  centers.

The frequency dependence of tangent of dielectric losses  $\tan\delta$  (Fig. 4) is a curve with a maximum of around  $10^5$  Hz at room temperature. The peak on the curve is caused by the reorientation of dipoles. A weak maximum of around  $10^3$  Hz is also observed (Fig. 4). As the temperature falls, both maxima move to the low-frequency range. The activation energy of dipole rotation is 0.58 eV (insert in Fig. 4). This energy is logically associated with the energy of the migration of anion vacancies near  $\text{Yb}^{2+}$ .

## DISCUSSION

The increase in electrical conductivity with alternating current in  $\text{LaF}_3\text{-Yb}^{2+}$  crystals upon an increase in the  $\text{Yb}^{2+}$  concentration indicates that anion vacancies are charge-compensated defects in  $\text{Yb}^{2+}$ . The maximum of dielectric losses and the reduced frequency of the peak maximum as the temperature falls along with the activation energy (Fig. 4), which is close to the energy of migration of anion vacancies, indicate that  $\text{Yb}^{2+}$ -anion vacancies are created by the migration of vacancies upon the reorientation of dipoles. For  $\text{Sm}^{2+}$  and  $\text{Eu}^{2+}$  ions, the spectra of the dielectric losses of  $\text{LaF}_3$  show maxima associated with the reorientation of anion vacancies near impurity ions [5, 6]. The energies of reorientation for  $\text{RE}^{2+}$  dipoles in  $\text{LaF}_3$  are 0.48, 0.51, and 0.58 eV for  $\text{Sm}^{2+}$ ,

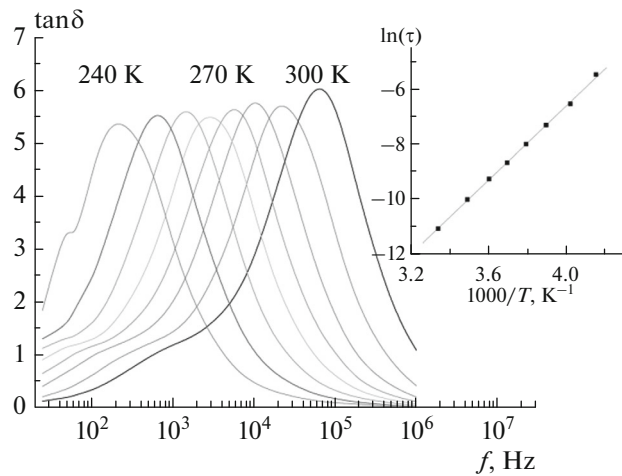


**Fig. 4.** Frequency dependence of tangent of dielectric losses  $\tan\delta$  of  $\text{LaF}_3\text{-0.3\% YbF}_3$  ( $\text{Yb}^{2+}$ ) crystals at different temperatures. The insert shows the correlation between the natural logarithm of the period of the reorientation of the dipole and reverse temperature (the Arrhenius plot), which allows us to determine the energy of dipole reorientation ( $E = 0.58 \pm 0.01$  eV).

$\text{Eu}^{2+}$ , and  $\text{Yb}^{2+}$ , respectively. The crystal radii of divalent ions shrink as the atomic number rises from Sm to Eu and Yb [13]. The drop in reorientation energy is probably due to the more compact lattice around impurity ions as their radii grow, which hampers vacancy migration.

The energy of  $4f^{14}\text{-}4f^{13}5d^1$  zero-phonon transitions for  $\text{Yb}^{2+}$  in  $\text{LaF}_3$  is 3.8 eV (326 nm), according to the semi-empirical Dorenbos model [14]. The position of the zero-phonon transitions for the absorption band at 370 nm can be estimated from the long-wave edge as 450 nm, while the corresponding wavelength for the absorption band at 304 nm is 320 nm (Figs. 1, 2). The accuracy of estimating the energies of transition according to the Dorenbos model is 0.1–0.2 eV [15]. We may therefore conclude that the band at 304 nm in  $\text{LaF}_3\text{-Yb}^{2+}$  is definitely caused by  $4f^{14}\text{-}4f^{13}5d^1$  transitions, while the long-wave band at 370 nm is of another origin.

On the basis of earlier results, we may conclude that the absorption spectra of  $\text{Sm}^{2+}$ -,  $\text{Eu}^{2+}$ - or  $\text{Yb}^{2+}$ -bearing  $\text{LaF}_3$  crystals contained two groups of bands. The long-wave bands at 550–650 ( $\text{Sm}^{2+}$ ) and 330–400 ( $\text{Eu}^{2+}$  and  $\text{Yb}^{2+}$ ) nm were caused by transitions from the  $4f^m$  ground state of impurity ions to the levels of charge-compensated anion vacancies. The short-wave absorption bands were caused by  $4f^n\text{-}4f^{n-1}5d^1$  transitions in impurity ions.

The shift of the long-wave absorption band toward low energies as the crystals cooled was observed not

only in LaF<sub>3</sub>–Yb<sup>2+</sup> (Fig. 1), but also in the LaF<sub>3</sub>–Sm<sup>2+</sup> and LaF<sub>3</sub>–Eu<sup>2+</sup> crystals. The long-wave shift of the maximum of the first absorption band upon cooling to 7.5 K was 0.11 eV for Sm<sup>2+</sup> and Eu<sup>2+</sup> and 0.06 eV for Yb<sup>2+</sup>. We may assume that at high temperatures, RE<sup>2+</sup> and vacancies converge due to Coulomb attraction, which raises the energy of electron transfer from RE ions to vacancies.

Down to 7 K, the excitation of Sm<sup>2+</sup>, Eu<sup>2+</sup>, and Yb<sup>2+</sup> ions in the long-wave absorption bands produces no luminescence. After electron-to-vacancy transfer, the positions of surrounding ions most likely relax strongly, due to the larger radii of vacancies with electrons and the reduced sizes of RE ions that have lost electrons. The difference between the energies of the ground and excited states at such positions of the lattice ions becomes very small, leading to radiation-free transitions or transitions in the IR-range with wavelengths of more than 1200 nm.

According to estimates, the 5*d*-levels of all divalent ions in an LaF<sub>3</sub> crystal fall into the conductivity band, which should not result in luminescence [14]. No luminescence of Sm<sup>2+</sup>, Eu<sup>2+</sup>, or Yb<sup>2+</sup> ions, which is caused by transitions from the 5*d*- to the 4*f*-states, is observed. Sm<sup>2+</sup> ions are characterized by excited 4*f*-states below the bottom of the conductivity band; this allowed us to observe the transitions from excited <sup>5</sup>D<sub>*j*</sub> (*j* = 0, 1, 2) states to states <sup>4</sup>F<sub>*i*</sub> (*i* = 0, 1, 2, 3, 4, 5) [4]. The wide structureless band of LaF<sub>3</sub>–Eu<sup>2+</sup> luminescence is caused by so-called anomalous luminescence (transitions from the bottom of the conductivity band to the 4*f*-level of Eu<sup>2+</sup>) [6]. The location of the excited level within the conductivity band is a necessary condition for anomalous luminescence that occurs for all divalent RE ions in LaF<sub>3</sub> [14]. However, the anomalous luminescence caused by transitions from the band to the ground state of trivalent RE ions was observed only for LaF<sub>3</sub>–Eu<sup>2+</sup> crystals [6]. No luminescence was observed in LaF<sub>3</sub>–Yb<sup>2+</sup> crystals upon the excitation of 4*f*<sup>14</sup>–4*f*<sup>13</sup>5*d*<sup>1</sup>-bands.

## CONCLUSIONS

As with Sm<sup>2+</sup> and Eu<sup>2+</sup> centers, the ground state of Yb<sup>2+</sup> centers in LaF<sub>3</sub> is described by the configuration of Yb<sup>2+</sup>-anion vacancies. The migration of vacancies near Yb<sup>2+</sup> result in conductivity with alternating current and of peak of dielectric losses with an energy of dipole reorientation of 0.58 eV.

The long-wavelength absorption band at 370 nm corresponds to transitions of electrons from the 4*f*<sup>14</sup>-level of Yb<sup>2+</sup> to anion vacancies, while other bands are caused by 4*f*<sup>14</sup>–4*f*<sup>13</sup>5*d*<sup>1</sup> transitions in Yb<sup>2+</sup> ions. No luminescence related to Yb<sup>2+</sup> centers was observed.

## ACKNOWLEDGMENTS

This work was performed using the scientific equipment at the Isotopic and Geochemical Studies Shared Resource Center of the Vinogradov Institute of Geochemistry. The authors thank V.A. Kozlovskii for growing our REE-doped LaF<sub>3</sub> crystals.

## REFERENCES

1. Carnall, W., Goodman, G.L., Rajnak, K., and Rana, R.S., *J. Chem. Phys.*, 1989, vol. 90, p. 3443.
2. Görlich, P., Karras, H., Kötz, G., and Lehmann, R., *Phys. Status Solidi (b)*, 1964, vol. 5, no. 3, p. 437; Görlich, P., Karras, H., Kötz, G., and Lehmann, R., *Phys. Status Solidi (b)*, 1964, vol. 6, no. 2, p. 277; Görlich, P., Karras, H., Kötz, G., and Lehmann, R., *Phys. Status Solidi (b)*, 1965, vol. 8, no. 2, p. 385.
3. Dieke, G.H., *Spectra and Energy Levels of Rare Earth Ions in Crystals*, New York: Interscience, 1968.
4. Radzhabov, E.A., *Opt. Spectrosc.*, 2016, vol. 121, no. 4, p. 482.
5. Radzhabov, E.A. and Kozlovskii, V.A., *Phys. Procedia*, 2015, vol. 76, p. 47.
6. Radzhabov, E.A. and Shendrik, R.Yu., *Radiat. Meas.*, 2016, vol. 90, p. 80.
7. Heaps, W.S., Elias, L.R., and Yen, W.M., *Phys. Rev. B*, 1976, vol. 13, p. 94.
8. Rast, H.E., Caspers, H.H., and Miller, S.A., *J. Chem. Phys.*, 1967, vol. 47, p. 3874.
9. Shcheulin, A.S., Angervaks, A.E., Semenova, T.S., et al., *Appl. Phys. B*, 2013, vol. 111, p. 551.
10. Ivanov-Shits, A.K. and Murin, I.V., *Ionika tverdogo tela (Solid-State Ionics)*, St. Petersburg: S.-Peterb. Gos. Univ., 2000.
11. Roos, A., Franceschetti, D., and Schoonman, J., *J. Phys. Chem. Solids*, 1985, vol. 46, p. 645.
12. Schönhals, A. and Kremer, F., in *Broadband Dielectric Spectroscopy*, Springer, 2003, p. 59.
13. Jia, Y.Q., *J. Solid State Chem.*, 1991, vol. 95, p. 184.
14. Dorenbos, P., *J. Lumin.*, 2013, vol. 135, p. 93.
15. Zych, A., Ogieglo, J., Ronda, C., et al., *J. Lumin.*, 2013, vol. 134, p. 174.

*Translated by I.Yu. Melekestseva*